Theoretical Insights into a CO Dimerization Mechanism in CO2 Electroreduction

ARTICLE *in* JOURNAL OF PHYSICAL CHEMISTRY LETTERS · MAY 2015

Impact Factor: 7.46 · DOI: 10.1021/acs.jpclett.5b00722

4 AUTHORS, INCLUDING:

Joseph H. Montoya
Lawrence Berkeley National Laboratory
12 PUBLICATIONS **67** CITATIONS
SEE PROFILE

Chuan Shi
Stanford University
7 PUBLICATIONS **49** CITATIONS
SEE PROFILE

Karen Chan
Stanford University
23 PUBLICATIONS **179** CITATIONS
SEE PROFILE

THE JOURNAL OF PHYSICAL CHEMISTRY Letters

Letter

pubs.acs.org/JPCL

Theoretical Insights into a CO Dimerization Mechanism in CO_2 Electroreduction

Joseph H. Montoya,[†] Chuan Shi,[†] Karen Chan,[†] and Jens K. Nørskov*[,†,‡]

[†]SUNCAT Center for Catalysis and Interface Science Department of Chemical Engineering, Stanford University, 443 Via Ortega, Stanford, California 94305, United States

[‡]SUNCAT Center for Catalysis and Interface Science, SLAC National Accelerator Laboratory, 2675 Sand Hill Road, Menlo Park, California 94025, United States

Supporting Information

ABSTRACT: In this work, we present DFT simulations that demonstrate the ability of Cu to catalyze CO dimerization in CO_2 and CO electroreduction. We describe a previously unreported CO dimer configuration that is uniquely stabilized by a charged water layer on both Cu(111) and Cu(100). Without this charged water layer at the metal surface, the formation of the CO dimer is prohibitively endergonic. Our calculations also demonstrate that dimerization should have a lower activation barrier on Cu(100) than Cu(111), which, along with a more exergonic adsorption energy and a corresponding higher coverage of *CO, is consistent with experimental observations that Cu(100) has a high activity for C−C coupling at low overpotentials. We also demonstrate that this effect is present with cations other than H^+, a finding that is consistent with the experimentally observed pH independence of C_2 formation on Cu.

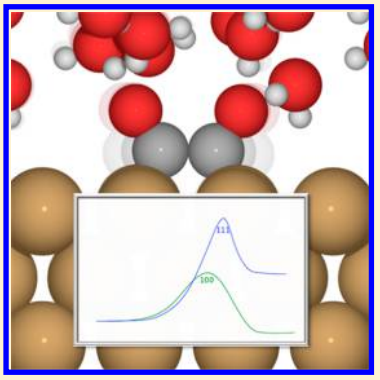

In recent years, CO_2 electroreduction has been a topic of considerable interest to both the scientific and energy technology communities, largely because it represents a potential route to both carbon-neutral fuel production and renewable feedstocks of carbon-based fine chemicals. Furthermore, many details of the catalysis of CO_2 electroreduction remain elusive. Among the most puzzling of these is the selectivity of copper metal catalysts to C_2 products like ethylene (C_2H_4). Although small amounts of C_2 products may form on other metal catalysts,[1] Cu is the only metal yet reported to convert CO_2 into ethylene at Faradaic efficiencies above 5%.[2−4] Furthermore, both Hori[4] and Schouten et al.[5−7] have shown that C_2 yields are pH dependent on an RHE scale, suggesting that a mechanism exists whose rate-determining step does not depend on a proton-coupled electron transfer (PCET). Yields of ethanol and ethylene on oxide-derived (OD) Cu from the work of Li et al.[8] and Kas et al.[9] at potentials less negative than −0.5 V vs RHE also suggest a low overpotential C−C coupling mechanism.

Schouten et al. proposed a CO dimerization mechanism to explain this trend in both CO_2 and CO electroreduction.[5] Previous theoretical studies, all performed at a vacuum-metal interface, have suggested that kinetic barriers to the formation of a C−C bond between unprotonated CO adsorbates on Cu surfaces are too high for the turnover of C_2 products at reasonable rates on Cu 211, even in the presence of applied electric fields likely to exist in electrochemical environments.[10] Calle-Vallejo et al.[11] suggested that barriers to CO dimerization with gas-phase precursors, i.e., with an Eley−Rideal mechanism, are not as high, but the exergonic binding energy of CO* on 211 steps and 100 terraces of Cu[12] suggests that adsorbed, rather than gas-phase CO is the relevant precursor to the kinetics of C−C coupling between CO species. In addition, this previous work also proposed a stabilization of the CO dimer and its transition state by scaling the energy using the number of excess electrons in the adsorbed species as determined from a Bader charge analysis. However, this approach to stabilizing the CO dimer and the associated transition state lacks the rigorous treatment of the electrochemical potential.[13] We comment further on this discrepancy in the Supporting Information.

In this work, we present theoretical evidence of a CO dimerization mechanism in an explicit electrochemical double layer on Cu(111) and Cu(100), and show that a combination of the resulting field and solvation effects significantly reduce both the thermodynamic and kinetic energy requirement for CO dimer formation from the relevant precursor, adsorbed CO*. We show that this effect occurs in the presence of a range of solvated cations in the water layer, suggesting that this stabilization occurs under an absolute potential, rather than on the RHE scale. Ultimately, these results demonstrate that the energetics of chemical steps under electrochemical conditions may deviate significantly from their counterparts in vacuum, and provide theoretical support for the dimerization of CO previously proposed by Schouten et al.[5]

Received: April 7, 2015
Accepted: May 1, 2015
Published: May 1, 2015

DOI: 10.1021/acs.jpclett.5b00722
J. Phys. Chem. Lett. 2015, 6, 2032−2037

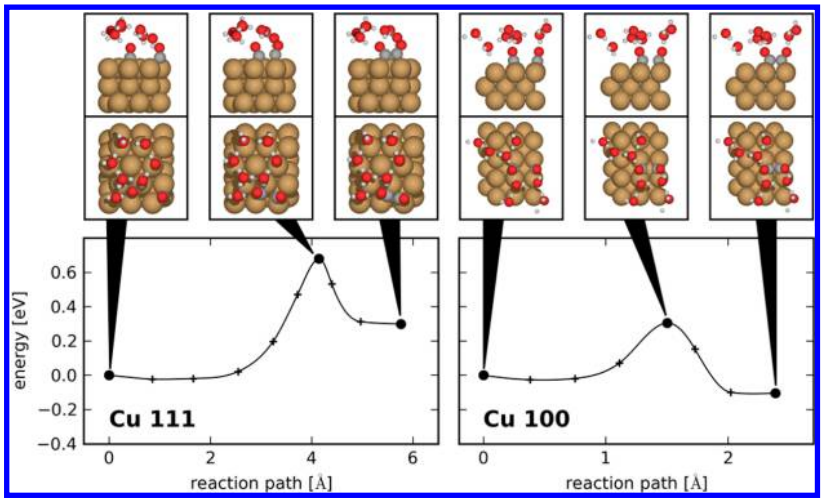

Figure 1. Kinetic barriers for the formation of a CO dimer from two adsorbed CO species for Cu(111) (left) and Cu(100) (right), calculated using the NEB method. The barriers of 0.68 (111) and 0.33 eV (100) that we find demonstrate that Cu(100) should form CO dimers at significantly higher rates than Cu(111). Also shown are visual schematics of the initial, transition, and final states for both calculations.

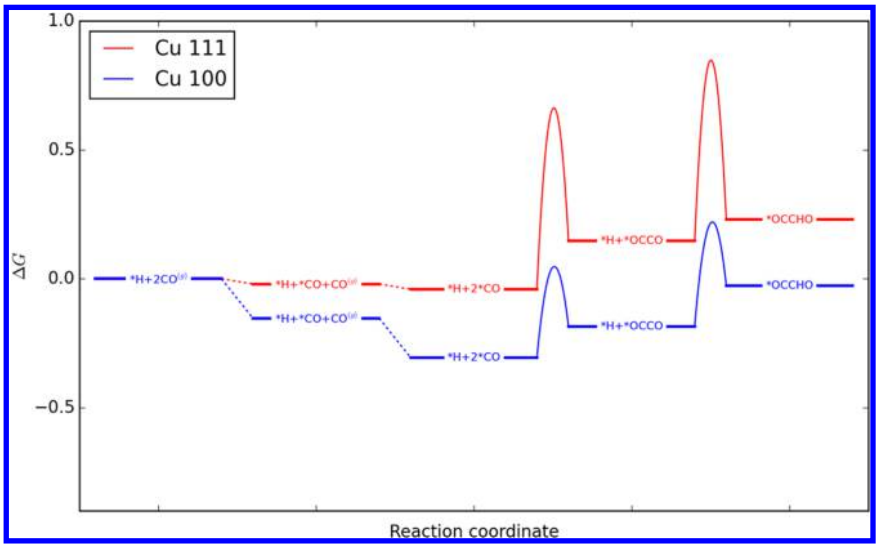

Figure 2. Free energy diagrams for the formation of *OCCHO from $CO^{(g)}$ and adsorbed hydrogen (*H) on Cu 100 and Cu 111. Elementary steps include the adsorption of two CO molecules to form *CO, the formation of a *CO dimer, and the hydrogenation of the *CO dimer.

The barriers for coupling between CO adsorbates on both the 111 and 100 surfaces were determined using nudged elastic band (NEB) calculations and are shown in Figure 1. Their corresponding values are 0.68 and 0.33 eV, respectively. As we discuss later, the work function of these structures do roughly correspond to the absolute potentials at relevant CO_2RR conditions in neutral or alkaline solutions. The activation energies reported in Figure 1 are significantly lower than either barrier of 1.5 eV previously reported on 211[10] or the barrier of 1.0 eV from Calle-Vallejo et al.,[11] using adsorbed *CO precursors and with no ad hoc stabilization. The explicit charged single layer of solvent, which is geometry optimized along with the adsorbates in the initial and final states for each reported NEB result, reduces the barrier such that it is well below the ∼0.75 eV barrier corresponding to a TOF of 1 s^{-1} from basic transition state theory,[14] and considered to be a threshold for fast kinetics.

A second key aspect of this result is that the 100 terrace is predicted to have a significantly lower barrier for dimerization of CO than the close-packed 111 surface. The lowering of this barrier by 0.3−0.4 eV on Cu 100 relative to Cu 111 corresponds to an increase in turnover frequency of at least 5 orders of magnitude. While the structure sensitivity described by this result is suggestive of a more active Cu 100 facet, as observed in experiment, dimer formation on Cu 111 is also predicted to be facile, but thermodynamically uphill from gas-phase CO.

We also examine the energetics one step further along the reaction path toward ethylene. Using the CHE and the same charged solvation environment used for the CO dimer, we predict that OCCHO* should be the most thermodynamically favorable state derived from a PCET to OCCO*. In addition, we find that the barrier of the surface hydrogenation of OCCO* to form OCCHO*, is 0.75 eV on Cu 111 and 0.38 eV on Cu 100. In Figure 2, we sketch a free energy diagram for the adsorption of CO*, the dimerization barrier reported in Figure 2, and the subsequent hydrogenation barrier on Cu 111 and Cu 100. Previous work suggests that hydrogenation and PCET steps proceeding from OCCHO en route to ethylene and

DOI: 10.1021/acs.jpclett.5b00722
J. Phys. Chem. Lett. 2015, 6, 2032−2037

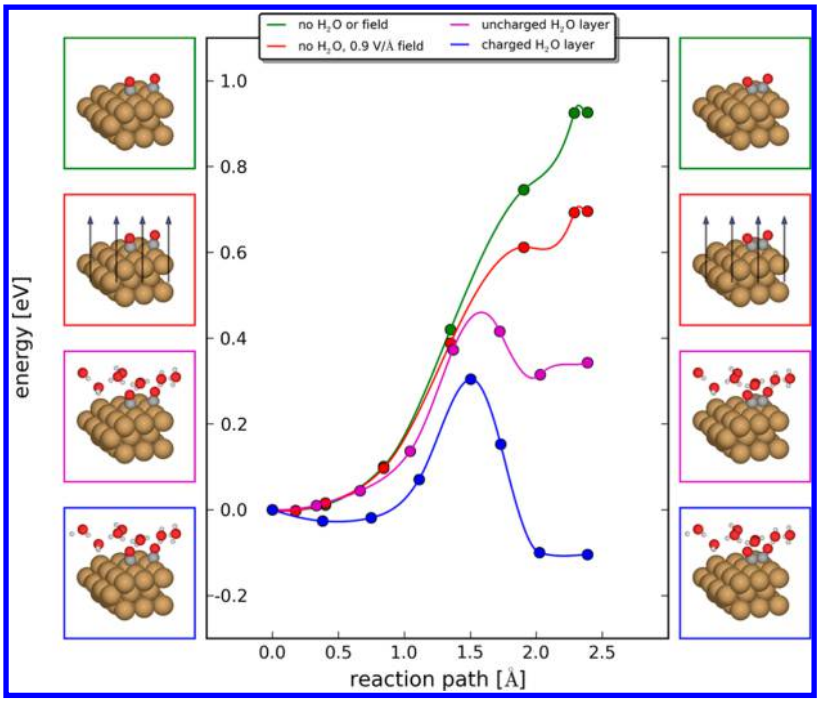

Figure 3. Energy barriers from solvation and field effects—energy profiles from single point calculations along the reaction path for CO dimerization on Cu 100 for field and solvation conditions. Approximate energy barriers from vacuum (green), i.e., no water or field, a uniform applied electric field of 0.9 V/Å (red), a single water layer (magenta), and a charged water layer (blue, as shown in Figure 2) are shown.

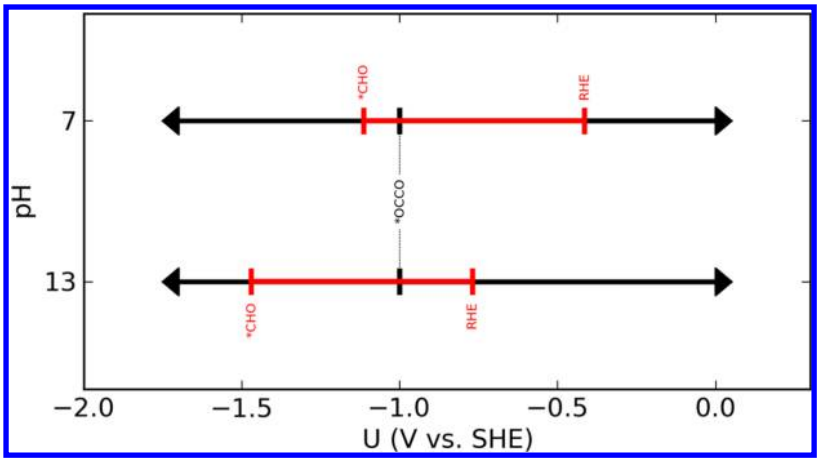

Figure 4. How onset via the *CO dimerization mechanism is fixed relative to SHE and becomes less negative versus RHE at higher pH. The *OCCO formation potential, −1.0 V vs SHE, is to the average potential corresponding to the work functions in Table 1. We note also that mechanisms that require *CHO as an intermediate[15] should be more well-differentiated at alkaline pH conditions.

ethanol are exergonic and likely do not impose further potential limitations.[10,11]

Our interpretation of the free energies reported in Figure 2 is twofold. First, the kinetics of CO conversion to ethylene along the CO dimerization pathway should depend on *CO binding energy, which should be higher on Cu(100) than Cu(111), since the *CO binding is more downhill by 0.2 eV, as shown in the figure. Second, the hydrogenation steps have significantly lower barriers on the 100 than the 111 facet, suggesting that the reduction pathway should be more favorable on 100. Determining quantitative turnovers to C_2 products may therefore require a very detailed kinetic model, since absolute rates likely depend on the C−C coupling barrier height, coverage of *H and *CO, and the PCET energetics as a function of both potential and pH. Since kinetic modeling is outside the scope of this work, we interpret our result to support the qualitative trend that Cu(100) is more active than Cu(111), which is consistent with experiment.

To determine more explicitly which aspects of the electrolyte affect the kinetic barrier for CO dimerization, we applied a uniform electric field and an explicit, uncharged solvent independently to the single points along the reaction coordinate. These results, shown in Figure 3, suggest that the local electric field can reduce the final state energy of the CO dimer by 0.2 eV, while the solvent stabilizes the dimer by 0.6 eV. Taken together, the results suggest that the CO dimer, and thus the transition state toward forming adsorbed OCCO*, are stabilized by a combined field and solvation effect that allows for a barrier low enough to correspond to fast kinetics at room

DOI: 10.1021/acs.jpclett.5b00722
J. Phys. Chem. Lett. 2015, 6, 2032−2037

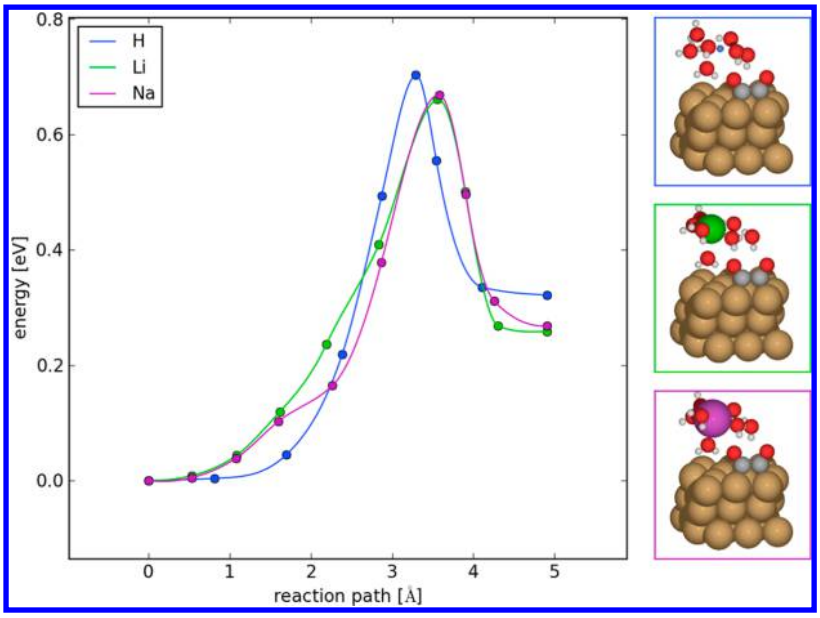

Figure 5. Energy barriers with different ions − NEB calculations for dimerization of adsorbed *CO with three different charged water layer on Cu 111. Results show barriers from charged water layer containing a proton (blue), a Li^+ ion (green), and a Na^+ ion (magenta).

temperature. Details on the electric field calculation are provided in the Supporting Information.

This interpretation is also consistent with the effect of C−C coupling at lower potentials in base. Field effects are likely functions of an absolute potential, i.e. referenced to a standard hydrogen electrode (SHE), rather than the reversible hydrogen electrode (RHE) scale typically used to present DFT calculations and to calculate theoretical overpotentials. If the onset of detectable turnover of ethylene, i.e., of the formation of a solvent orientation and ion concentration necessary to reduce the *CO dimerization barrier, is fixed vs SHE, then it becomes less negative on an RHE scale at higher pH. We outline this trend schematically in Figure 4. As shown in the figure, both the equilibrium potential for hydrogen evolution (i.e., 0 V vs RHE) and the potential at which *CHO formation from *CO shift upward on an SHE scale. The potential at which *OCCO, however, should not and therefore becomes less negative at pH 13 than at pH 7 on an RHE scale.

To further illustrate that our results suggest that the barrier reduction is a function of absolute, rather than relative potential, we present a set of barriers calculated using ions other than protons, the local concentration of which might be affected by the pH. In Figure 5, we compare the barriers for *CO dimerization in the presence of a charged water layer containing an extra hydrogen, lithium, and sodium atom. The barriers for these three cases vary by less than 0.1 eV, suggesting that the kinetics coupling of *CO coupling are enhanced in the presence of of solvated cations other than H_3O^+.

In these simulations, a work function can be calculated to provide a basis for comparing the potentials present in our calculations to experiment. We note that it is possible to determine barriers at constant potential using a series of larger and larger unit cells, as done in Skulason et al.[16] However, here the initial and final states are used as a rough estimate of the corresponding potential of the calculated barrier to illustrate the predicted trends in pH. In the case of solvated H_3O^+, we have initial and final work functions of 3.1 and 4.0 eV, as shown in Table 1 below. Assuming the reported experimentally

Table 1. Work Function Data for Simulated Electrode−Electrolyte Interface on Cu(111)

configuration	initial	final	U vs SHE	U vs RHE (pH = 7)	U vs RHE (pH = 13)
solvated H^+	3.1	4.0	[−1.3,−0.4]	[−0.9,+0.0]	[−0.5,+0.5]
solvated Li^+	2.6	3.5	[−1.8,−0.9]	[−1.4,−0.5]	[−1.0,+0.0]
solvated Na^+	2.7	3.7	[−1.7,−0.7]	[−1.3,−0.3]	[−0.9,+0.1]

determined SHE work function of 4.4 eV,[17] our simulated potential is −1.3 V vs SHE in the initial state and evolves to −0.4 V vs SHE in the final state. At pH 0, the RHE values corresponding to these potentials would be identical to SHE, suggesting that the solvent and ion configurations necessary to allow for low CO coupling barriers may not occur in those conditions. In base, however, the RHE potentials corresponding to these absolute potentials are much less negative, and can be calculated using the Nernst equation, as shown in Table 1.[18] In particular, at pH 7, we have a starting potential of −0.9 V vs RHE and final potential of +0.0 V vs RHE, which suggests that CO dimerization may begin at potentials prior to the typically measured onset of ethylene production at around −0.8−0.9 V vs RHE at this pH. Alkaline solutions should have an even lower onset of this effect, and the work functions we report correspond to −0.5 and 0.5 V vs RHE for pH 13 in the initial and final geometries, respectively. While these results may not accurately identify the earliest possible onset of C−C coupling, they are consistent with the potentials at which Schouten et al.'s observations of ethylene, which produce a peak detection of ethylene at −0.6 and −0.4 at pH 7 and 13, respectively.

In summary, we offer an explanation for the low overpotential C−C coupling observed on Cu 100 that shifts toward a less negative onset at high pH on an RHE scale. Our calculations show that CO dimers form with low barriers in the presence of a single layer of charged electrolyte, and do so with particularly low barriers on Cu(100). Surface hydrogenation may also be relevant to the overall kinetics, and further distinguish the activity between the two facets, since the barriers are 0.4 eV higher to hydrogenate *OCCO on Cu(111)

DOI: 10.1021/acs.jpclett.5b00722
J. Phys. Chem. Lett. 2015, 6, 2032−2037

than Cu(100). The reduction of the kinetic barrier for CO dimer formation seems to be a combined effect of solvation and local electric field. Since this effect can be induced not only by protons in the electrochemical double-layer, but also by Li^+ and Na^+, our results are consistent with the onset of *CO dimerization occurring on an absolute potential scale. Lastly, the associated work functions calculated in our simulations correlate with experimentally observed onset potentials for ethylene detection on Cu 100 in base, suggesting that the physics we describe herein should be applicable at the relevant experimental conditions.

COMPUTATIONAL METHODS

In this work, we use density functional theory (DFT) to determine the electronic energies of intermediates along a reaction pathway from two dissociated, adsorbed CO molecules to a CO dimer adsorbed on a Cu 111 surface. A 4 × 3 × 3 supercell of fcc Cu 111 and 100 with a single layer of eight water molecules at the surface was constructed to model the electrode−electrolyte interface. We determined optimal water layer structures using a minima-hopping algorithm that alternatively uses simulated annealing and geometry optimization approach to construct a series of local minima,[19] and chose the most favorable configuration to find a reaction path for CO dimerization. The water structure determined using this method closely resembles the hexagonal ice-like structure used previously in various DFT-based studies of adsorption and PCET kinetics on Pt 111.[20,21] Details concerning the water structure, adsorption energies, and free energy corrections are provided in the ESI.

To simulate the charged double layer at the electrode−electrolyte interface at reducing potentials, a single hydrogen or alternate alkali metal atom was placed into the near-surface water layer. The ground-state electronic structure of this configuration (as solved using the above methods) redistributes the charge from this atom's one electron to give it a cationic character and allow for the charge-separated double layer that simulates the electrochemical interface. To estimate the potential range of the calculations shown, a work function for each intermediate state was calculated and compared to previous literature values corresponding to values for the potential vs SHE.[17,22]

ASSOCIATED CONTENT

Supporting Information

Calculation parameters, details concerning the formulation of the electrochemical potential, and thermodynamic data are provided in the Supporting Information. The Supporting Information is available free of charge on the ACS Publications website at DOI: 10.1021/acs.jpclett.5b00722.

AUTHOR INFORMATION

Notes

The authors declare no competing financial interest.

ACKNOWLEDGMENTS

The authors acknowledge support from the MURI collaboration under AFOSR Award No. FA9550-10-1-0572. In addition, J.H.M. acknowledges support from the NSF GFRP, Grant Number DGE-114747.

REFERENCES

(1) Hatsukade, T.; Kuhl, K. P.; Cave, E. R.; Abram, D. N.; Jaramillo, T. F. Insights Into the Electrocatalytic Reduction of CO_2 on Metallic Silver Surfaces. *Phys. Chem. Chem. Phys.* **2014**, *16*, 13814−13819.
(2) Kuhl, K. P.; Hatsukade, T.; Cave, E. R.; Abram, D. N.; Kibsgaard, J.; Jaramillo, T. F. Electrocatalytic Conversion of Carbon Dioxide to Methane and Methanol on Transition Metal Surfaces. *J. Am. Chem. Soc.* **2014**, *136*, 14107−14113.
(3) Kuhl, K. P.; Cave, E. R.; Abram, D. N. New Insights Into the Electrochemical Reduction of Carbon Dioxide on Metallic Copper Surfaces. *Energy Env. Sci.* **2012**, *5*, 7050−7059.
(4) Hori, Y. Electrochemical CO_2 Reduction on Metal Electrodes. In *Modern Aspects of Electrochemistry*; Springer New York: New York, 2008; Vol. *42*, pp 89−189.
(5) Schouten, K.; Kwon, Y.; Van der Ham, C.; Qin, Z. A New Mechanism for the Selectivity to C1 and C2 Species in the Electrochemical Reduction of Carbon Dioxide on Copper Electrodes. *Chem. Sci.* **2011**, *2*, 1902−1909.
(6) Schouten, K. J. P.; Gallent, E. P.; Koper, M. T. M. Structure Sensitivity of the Electrochemical Reduction of Carbon Monoxide on Copper Single Crystals. *ACS Catal.* **2013**, *3*, 1292−1295.
(7) Schouten, K. J. P.; Qin, Z.; Gallent, E. P.; Koper, M. T. M. Two Pathways for the Formation of Ethylene in CO Reduction on Single-Crystal Copper Electrodes. *J. Am. Chem. Soc.* **2012**, *134*, 9864−9867.
(8) Li, C. W.; Ciston, J.; Kanan, M. W. Electroreduction of Carbon Monoxide to Liquid Fuel on Oxide-Derived Nanocrystalline Copper. *Nature* **2014**, *508*, 504−507.
(9) Kas, R.; Kortlever, R.; Milbrat, A.; Koper, M. T. M.; Mul, G.; Baltrusaitis, J. Electrochemical CO_2 Reduction on Cu_2O-Derived Copper Nanoparticles: Controlling the Catalytic Selectivity of Hydrocarbons. *Phys. Chem. Chem. Phys.* **2014**, *16*, 12194−12201.
(10) Montoya, J. H.; Peterson, A. A.; Nørskov, J. K. Insights Into C−C Coupling in CO_2 Electroreduction on Copper Electrodes. *ChemCatChem* **2013**, *5*, 737−742.
(11) Calle-Vallejo, F.; Koper, M. T. M. Theoretical Considerations on the Electroreduction of CO to C_2 Species on Cu(100) Electrodes. *Angew. Chem.* **2013**, *125*, 7423−7426.
(12) Durand, W. J.; Peterson, A. A.; Studt, F.; Abild-Pedersen, F.; Nørskov, J. K. Structure Effects on the Energetics of the Electrochemical Reduction of CO_2 by Copper Surfaces. *Surf. Sci.* **2011**, *605*, 1354−1359.
(13) Nørskov, J. K.; Rossmeisl, J.; Logadottir, A. Origin of the Overpotential for Oxygen Reduction at a Fuel-Cell Cathode. *J. Phys. Chem. B* **2004**, *108*, 17886−17892.
(14) Nørskov, J. K.; Studt, F.; Abild-Pedersen, F.; Bligaard, T. *Fundamental Concepts in Heterogeneous Catalysis*; John Wiley & Sons, Inc: Hoboken, NJ, 2014.
(15) Peterson, A. A.; Abild-Pedersen, F.; Studt, F.; Rossmeisl, J.; Nørskov, J. K. How Copper Catalyzes the Electroreduction of Carbon Dioxide Into Hydrocarbon Fuels. *Energy Environ. Sci.* **2010**, *3*, 1311−1315.
(16) Skulason, E.; Karlberg, G. S.; Rossmeisl, J.; Bligaard, T.; Greeley, J.; Jonsson, H.; Nørskov, J. K. Density Functional Theory Calculations for the Hydrogen Evolution Reaction in an Electrochemical Double Layer on the Pt(111) Electrode. *Phys. Chem. Chem. Phys.* **2007**, *9*, 3241−3250.
(17) Kötz, E. R.; Neff, H.; Müller, K. A. UPS, XPS and Work Function Study of Emersed Silver, Platinum and Gold Electrodes. *J. Electroanal. Chem. Int. Chem.* **1986**, *215*, 331−344.
(18) Bard, A. J.; Faulkner, L. R. *Electrochemical Methods: Fundamentals and Applications*; John Wiley & Sons: West Sussex, U.K., 1980.
(19) Peterson, A. A.; Abild-Pedersen, F.; Studt, F.; Rossmeisl, J.; Nørskov, J. K. How Copper Catalyzes the Electroreduction of Carbon Dioxide Into Hydrocarbon Fuels. *Energy Environ. Sci.* **2010**, *3*, 1311−1315.
(20) Gohda, Y.; Schnur, S.; Groß, A. Influence of Water on Elementary Reaction Steps in Electrocatalysis. *Faraday Discuss.* **2009**, *140*, 233−244.

DOI: 10.1021/acs.jpclett.5b00722
J. Phys. Chem. Lett. 2015, 6, 2032−2037

(21) Bondarenko, A. S.; Stephens, I. E. L.; Hansen, H. A.; Pérez-Alonso, F. J.; Tripkovic, V.; Johansson, T. P.; Rossmeisl, J.; Nørskov, J. K.; Chorkendorff, I. The Pt(111)/Electrolyte Interface Under Oxygen Reduction Reaction Conditions: An Electrochemical Impedance Spectroscopy Study. *Langmuir* **2011**, *27*, 2058−2066.
(22) Randles, J. E. B. The Real Hydration Energies of Ions. *Trans. Faraday Soc.* **1956**, *52*, 1573−1581.

DOI: 10.1021/acs.jpclett.5b00722
J. Phys. Chem. Lett. 2015, 6, 2032−2037